Title
Temperature dependent thermal conductivity of pure silica MEL and MFI zeolite thin films

Journal
Journal of Applied Physic, 111(5)

Authors
Fang, Jin
Huang, Yi
Lew, Christopher M.
et al.

Publication Date
2012-03-08

Peer reviewed

Journal of Applied Physics, Vol.111, pp.054910, 2012.

TEMPERATURE DEPENDENT THERMAL CONDUCTIVITY OF PURE SILICA MEL AND MFI ZEOLITE THIN FILMS

Jin Fang, Yi Huang, Laurent Pilon*
University of California, Los Angeles
Henry Samueli School of Engineering and Applied Science
Mechanical and Aerospace Engineering Department
420 Westwood Plaza, Los Angeles, CA 90095, USA
Email: pilon@seas.ucla.edu

Yushan Yan†
Department of Chemical Engineering
University of Delaware
150 Academy Street, Newark, Delaware 19716, USA
Email: yanys@udel.edu

Christopher M. Lew
Department of Chemical Engineering and Materials Science
University of Minnesota
Minneapolis, Minnesota 55455, USA

ABSTRACT

This paper reports the temperature dependent cross-plane thermal conductivity of pure silica zeolite (PSZ) MFI and MEL thin films measured using the 3ω method between 30 and 315 K. PSZ MFI thin films were b-oriented, fully crystalline, and had a 33% microporosity. PSZ MEL thin films consisted of MEL nanoparticles embedded in a non-uniform and porous silica matrix. They featured porosity, relative crystallinity, and particle size ranging from 40% to 59%, 23% to 47%, and 55 to 80 nm, respectively. Despite their crystallinity, MFI films were found to have thermal conductivity smaller than that of amorphous silica due to strong phonon scattering by micropores. In addition, the effects of increased relative crystallinity and particle size on thermal conductivity of MEL thin films were compensated by the simultaneous increase in porosity. Finally, thermal conductivity of MFI zeolite was predicted and discussed using the Callaway model based on the Debye approximation.

*Address all correspondence to this author.
†Address all correspondence to this author.

1 Introduction

Zeolites are a group of nanoporous crystalline aluminosilicates with uniform micropores. They differ by their crystalline structure, microporosity, and their framework density defined as the number of tetrahedrally coordinated atoms per 1000 $Å^3$. For example, the MFI structure has 0.55 nm wide sinusoidal channels along the *a*-axis and 0.53 nm wide straight channels along the *b*-axis [1]. The MEL structure has 0.54 nm wide straight channels along both the *a*- and *b*-axis [1]. The presence of these micropores contributes to the so-called microporosity. The framework density of PSZ MEL and MFI is 17.4 and 18.4, respectively [1]. Pure silica zeolites (PSZs) have no aluminum in their framework.

Zeolites have been considered as adsorbents for sorption-based heat exchangers for heat recovery and cooling applications [2–5]. They are also of interest for hydrogen storage as molecular sieves and as low-dielectric constant materials for very large scale integrated circuits [1, 6]. In addition, there is an emerging trend to use zeolite thin films in various micro/nanoscale applications, such as filters for air pollutants, microreactors, and miniature gas sensors [7–11]. In all these applications, knowledge of thermal properties of zeolites over a wide range of temperature is of significant importance for their practical implementation in devices and systems.

Several studies have reported the thermal conductivity of powdered zeolites [12–15]. Effects of temperature, filling gas, moisture, and pressure were investigated [12–15]. In addition, Greenstein *et al*. [16] and Hudiono *et al*. [17] measured thermal conductivity of PSZ MFI zeolite films with thickness ranging from 10 to 20 μm and temperature varying from 150 to 450 K. The MFI films were synthesized by secondary growth through a seeded hydrothermal process on alumina substrates. The measured thermal conductivity of (*h0l*)-oriented PSZ MFI films varied from 1.0 to 1.4 W/m·K in the temperature range considered [17]. That of calcined and uncalcined *c*-oriented PSZ MFI films deposited on silicon substrates was found to range from 0.75 to 1.1 W/m·K and 1.0 to 1.6 W/m·K, respectively [16]. More recently, Coquil *et al.* [18] measured room temperature thermal conductivity of PSZ MFI and MEL zeolite thin films. The MFI thin films were *b*-oriented, fully crystalline, and had a porosity of 33%. The MEL thin films featured porosity, relative crystallinity, and particle size ranging from 40% to 59%, 23% to 47%, and 55 to 80 nm, respectively. The authors found the thermal conductivity to be around 1.02±0.10 W/m·K for all films despite their different porosity, relative crystallinity, and nanoparticle size.

2 Methods and Experiments

2.1 Sample film preparation

Synthesis of PSZ MFI and MEL thin films investigated in the present study were previously described in detail [1, 6, 18]. MFI thin films were synthesized by *in situ* crystallization and were *b*-oriented. The MEL films were prepared by spin coating a zeolite nanoparticle suspension onto silicon substrates. The MEL suspension was synthesized by a two-stage process [1]. The first stage consisted of a 2 days heating and stirring of a tetraethylorthosilicate (TEOS) based solution at 80°C resulting in a MEL nanoparticle suspension. The second stage corresponded to the growth of the MEL nanoparticles from the same solution in a convection oven at 114°C. Finally, MEL thin films were obtained by spin-coating the solution onto silicon substrates. Both relative crystallinity and nanoparticle size of the PSZ MEL increased as the second stage synthesis time increased. Here, the relative crystallinity is defined as the ratio of the micropore volume to the micropore volume of a fully crystalline PSZ MEL microcrystal [1]. Four different sets of MEL films corresponding to four different second stage synthesis times (15, 18, 21 and 24 hours) were studied. Note that all the MEL and MFI thin films were made hydrophobic by vapor-phase silylation with trimethylchlorosilane as described in Ref. [1].

2.2 Characterization

Detailed characteristics of the resulting PSZ MFI and MEL thin films have been reported in the literature [1, 6, 19, 20]. Table 1 summarizes the characteristics of five types of PSZ MFI and

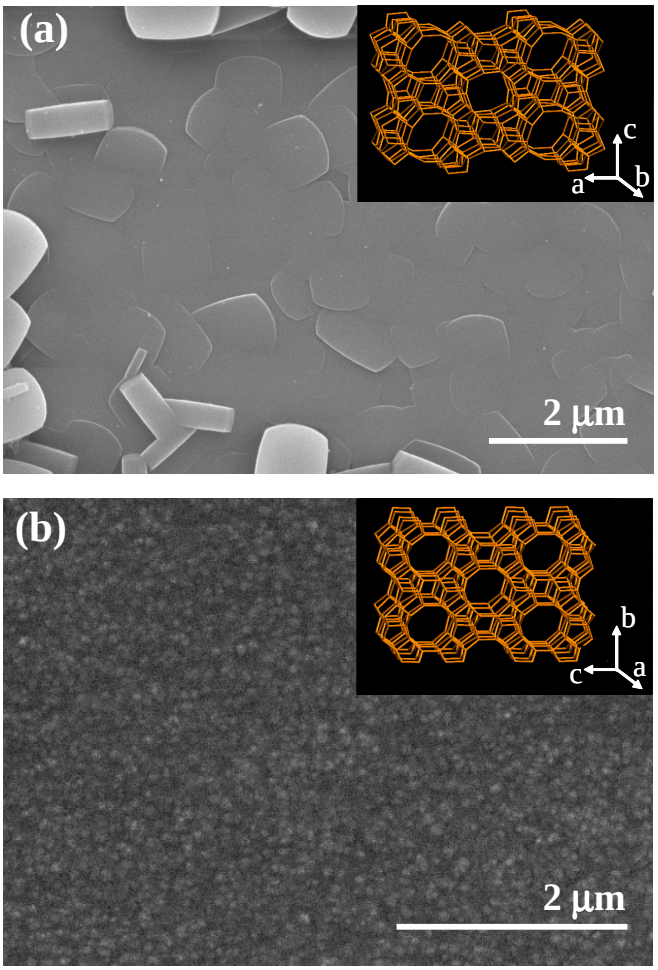

FIGURE 1. (Color online) SEM images of (a) *in situ* PSZ MFI and (b) spin-on MEL thin films. Insets show (a) the MFI framework viewed down the *b*-axis and (b) the MEL framework viewed down the *a*-axis [18].

MEL thin films investigated. Figure 1(a) shows a SEM image of an *in situ* PSZ MFI film (type 1) consisting of well-intergrown MFI crystals along with an inset showing the MFI framework viewed down the *b*-axis [18]. Figure 1(b) shows a SEM image of a spin-on PSZ MEL film (type 5) consisting of MEL nanoparticles embedded in a nonuniform, disordered, and porous silica matrix along with an inset showing the MEL framework viewed down the *a*-axis [18]. In addition, unlike the MFI thin film, the MEL thin films featured also a mesoporosity corresponding to the volume fraction occupied by mesopores 2.3 to 2.6 nm in diameter [21]. These mesopores were located between the disordered silica matrix and the MEL nanoparticles [22].

TABLE 1. Physical characteristics of the synthesized PSZ MFI and MEL thin films.

Sample type	Structure	Second stage duration (h)	MEL particle size (±1 nm)	Porosity (± 2%)	Total pore vol. (cm^2g^{-1})	Micropore vol. (cm^3g^{-1})	BET surface area (m^2g^{-1})	Micropore area (m^2g^{-1})	Thickness (±10 nm)	Relative crystallinity (± 2%)
1	MFI	-	-	33%[1]	0.19[2]	0.19[2]	457[2]	457[2]	320	100%
2	MEL	15	55	40%	0.60[3]	0.033[3]	691[3]	86[3]	350	23%[3]
3	MEL	18	60	45%	0.70[3]	0.048[3]	750[3]	119[3]	300	33%[3]
4	MEL	21	70	58%	0.80[3]	0.060[3]	852[3]	143[3]	280	44%[3]
5	MEL	24	80	59%	0.83[3]	0.068[3]	889[3]	149[3]	330	47%[3]

[1]From Flanigen *et al*. [19]
[2]From Tang *et al*. [20]
[3]Interpolated from Li *et al*. [1]

2.3 Thermal conductivity measurements

The cross-plane thermal conductivity of PSZ thin films was measured using the 3ω method [23, 24]. The principles, experimental apparatus, experimental procedure, and validation of the method have already been described elsewhere [25]. The experimental uncertainty typically varied from 5% to 10% corresponding to 95% confidence interval. The thermal conductivity of two different samples for each type of film listed in Table 1 was measured between 30 and 315 K. The measurements agreed within 10% of each other. In addition, the film thickness had negligible effect on the measured data. This can be attributed to the fact that phonon scattering by nanopores and crystal grain boundary dominated over phonon scattering by film boundary in PSZ films.

3 Physical Modeling

Finally, thermal conductivity of the PSZ MFI film was modeled using the following expression derived by Callaway [26],

$$k = \frac{k_B}{2\pi^2 v_g}\left(\frac{k_B T}{\hbar}\right)^3 \int_0^{\theta_D/T} \tau_{eff}(\omega)\frac{x^4 e^x}{(e^x-1)^2}dx, \qquad (1)$$

where k_B is the Boltzmann constant, $\hbar$ is the reduced Planck's constant, θ_D is the Debye temperature for MFI zeolite reported to be 377.6 K [27], $\tau_{eff}(\omega)$ is the effective phonon relaxation time, and v_g is the average effective sound velocity in MFI reported to be 3683 m/s [28]. The variable x is related to the phonon frequency ω and is equal to $\hbar\omega/k_BT$. Note that Equation (1) was obtained by using the Debye dispersion relation and density of states and ignoring the effect of phonon polarization as discussed in Ref. [29].

The effective phonon relaxation time τ_{eff} is related to the relaxation times for defect scattering τ_D, Umklapp scattering τ_U, and boundary scattering τ_B via the Matthiessen's rule as [26],

$$\frac{1}{\tau_{eff}} = \frac{1}{\tau_D} + \frac{1}{\tau_U} + \frac{1}{\tau_B}. \qquad (2)$$

Defect scattering refers to phonon scattering by point defects such as inclusion of impurity atoms or lattice vacancies [30]. Boundary scattering corresponds to phonon scattering by the film boundaries as well as by micropores. Here, τ_D, τ_U, and τ_B were expressed as [17, 30],

$$1/\tau_D = A\omega^4,\ 1/\tau_U = BT\omega^2\exp(-\theta_D/3T),\ \text{and}\ 1/\tau_B = v_g/l_B, \qquad (3)$$

where A and B are empirical constants, and l_B is the effective phonon mean free path (MFP) for boundary scattering.

4 Results and Discussion

4.1 Experimental results

Figure 2 shows the measured thermal conductivity of the PSZ MFI and MEL zeolite thin films as a function of temperature, along with data reported in the literature for calcined and uncalcined MFI zeolite [16] and amorphous silica [31]. The four MEL thin films differ from one another by their relative crystallinity. The inset shows a close view for the measured data for temperature $T > 150$ K in linear scale. The thermal conductivity of the *in situ* MFI film increased from 0.05 to 1.2 W/m·K as temperature increased from 30 to 315 K. In addition, it was about 10% to 15% larger than that of calcined MFI zeolite measured by Greenstein *et al*. [16] between 150 and 315 K. However, the thermal conductivity of uncalcined MFI [16] was about 20% to 40% larger than that measured in the present study [16]. This was likely due to the fact that the uncalcined films measured by

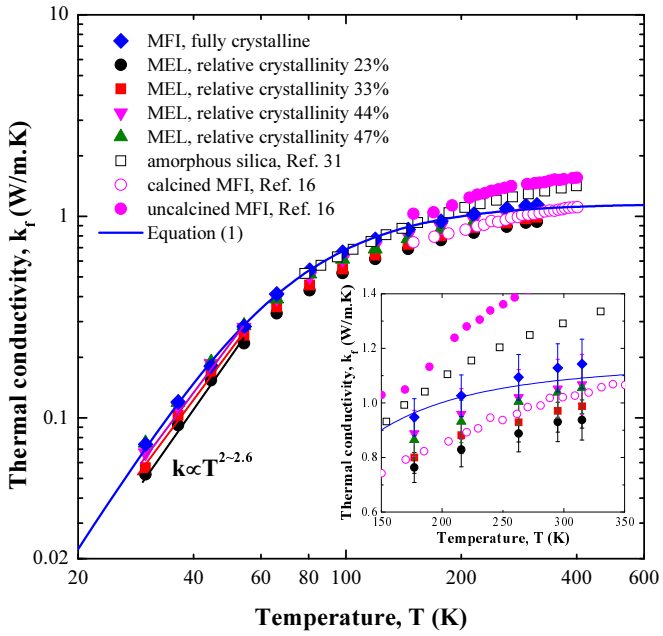

FIGURE 2. (Color online) Measured thermal conductivity of PSZ MFI and MEL zeolite thin films as a function of temperature from 30 to 315 K, along with data reported in the literature for calcined and uncalcined MFI zeolite [16] and amorphous silica [31]. The blue line indicates calculated thermal conductivity using the Callaway model [Equation (1)]. The inset shows a close view for the measured data for temperatures $T > 150$ K in linear scale.

Greenstein *et al.* [16] were denser (2.1 g/cm^3) than the *in situ* MFI film (1.7 g/cm^3) investigated in the present study. Moreover, the measured thermal conductivity of our MFI films was comparable to or smaller than that of the amorphous silica [31] despite its crystalline nature. In fact, the MFI films had microporosity of about 33% due to the presence of subnanometer pores within the crystalline structures. Its thermal conductivity was thus greatly reduced by phonon scattering by micropores.

In addition, Figure 2 indicates that all measured thermal conductivity k was linearly proportional to T^n with n varying from 2 to 2.6 for temperature $T < 60$ K. At low temperatures, strongly disordered materials typically follows $k \propto T^2$ while for crystalline materials $k \propto T^3$ [30]. The present results can be attributed to the fact that the MFI and MEL films featured crystalline nanostructures which were highly disordered due to the large surface area of pores and nanocrystals.

Furthermore, the inset in Figure 2 shows that the thermal conductivity of the PSZ MEL thin films was slightly smaller than that of the PSZ MFI thin film. This is due to the fact that the MEL thin films had larger porosity and were "partially" crystalline, consisting of crystalline nanoparticles embedded in amorphous silica matrix. Moreover, the thermal conductivity of MEL thin films increased slightly when the MEL relative crystallinity and particle size increased from 23% to 44% and 55 to 70 nm, respectively. However, it remained nearly unchanged when the relative crystallinity and particle size further increased beyond 44% and 70 nm. Then, the effects of increased relative crystallinity and particle size were compensated by the simultaneous increase in porosity.

4.2 Modeling results

By analogy with other studies [14, 16, 17, 30, 32], the parameters $A = 1.38 \times 10^{-42}$ s^3, $B = 4.24 \times 10^{-21}$ s/K, and $l_B = 0.95$ nm in Equation (3) were obtained by fitting the predictions of Equations (1) to (3) to the experimental data over the entire temperature range explored.

Figure 2 shows that the calculated thermal conductivity from Equations (1) to (3) agreed within 6% of the experimental data for the PSZ MFI film for all temperatures between 30 and 315 K. It establishes that using the Debye dispersion relation instead of the complete phonon dispersion was sufficient to predict the thermal conductivity of MFI zeolite films. In addition, phonon boundary scattering was found to dominate over phonon Umklapp scattering in MFI zeolite as discussed in the literature [14, 16–18]. In fact, the predicted thermal conductivity was insensitive to the Umklapp scattering relaxation time τ_U since $\tau_U \gg \tau_B$ and $\tau_U \gg \tau_D$ for all temperatures considered and all phonon frequencies up to the Debye cut-off frequency of $\omega_D/2\pi = 8$ THz. Similar conclusions were reached by Hudiono *et al.* [17] and Greenstein *et al.* [32] for MFI and LTA zeolite between 150 and 450 K.

Moreover, phonon defect scattering should be considered along with boundary scattering in order to accurately predict the thermal conductivity of the MFI films particularly at high temperatures. This was due to the fact that defect scattering strongly affects high frequency phonons ($1/\tau_D \propto \omega^4$) which contribute significantly to energy transport particularly at high temperatures [30]. At low temperatures, however, defect scattering was less important and boundary scattering dominated.

Finally, the fitted phonon boundary scattering MFP $l_B = 0.95$ nm was comparable with the distance between two adjacent micropores or the wall thickness. In fact, the lattice constant of MFI zeolite was reported to be about 2 nm along both a- and b- axis [33]. Considering the pore width of 0.55 nm along the a-axis and 0.53 nm along the b-axis [1], the wall thickness was estimated to be about 1.5 nm. Note that Hudiono *et al.* [17] reported a fitted value of $l_B = 4.8$ nm for MFI zeolite, also comparable with the wall thickness. The difference between l_B and MFI wall thickness may be attributed to the semi-empirical relaxation time models as well as the differences between Debye and actual phonon dispersion and density of states in MFI zeolite.

5 Conclusion

This paper reports the temperature dependent cross-plane thermal conductivity of PSZ MEL and MFI thin films. Despite their crystallinity, MFI thin films were found to have thermal conductivity comparable to or smaller than that of amorphous silica due to strong phonon scattering by micropore boundaries. For PSZ MEL films, effects of increased relative crystallinity and size of MEL nanoparticle on the thermal conductivity were compensated by the simultaneous increase in porosity. Finally, the thermal conductivity for MFI films was successfully modeled using the Callaway model based on the Debye approximation. Umklapp scattering had negligible effect on the predicted thermal conductivity. Instead, phonon boundary scattering dominated for all temperatures while defect scattering was important at high temperatures.

REFERENCES

[1] Li, Z., Lew, C., Li, S., Medina, D., and Yan, Y., 2005. "Pure-silica-zeolite MEL low-k films from nanoparticle suspensions". *Journal of Physical Chemistry B,* ***109***(18), pp. 8652–8658.

[2] Dieng, A., and Wang, R., 2001. "Literature review on solar adsorption technologies for ice-making and air-conditioning purposes and recent developments in solar technology". *Renewable and Sustainable Energy Reviews,* ***5***(4), pp. 313 – 342.

[3] Gordon, J., Ng, K., Chua, H., and Chakraborty, A., 2002. "The electro-adsorption chiller: A miniaturized cooling cycle with applications to micro-electronics". *International Journal of Refrigeration,* ***25***(8), pp. 1025–1033.

[4] Munoz, R. A., Beving, D., and Yan, Y., 2005. "Hydrophilic zeolite coatings for improved heat transfer". *Industrial and Engineering Chemistry Research,* ***44***(12), pp. 4310–4315.

[5] Liu, J., Aguilar, G., Munoz, R., and Yan, Y., 2008. "Hydrophilic zeolite coatings for improved heat transfer: A quantitative analysis". *AIChE Journal,* ***54***(3), pp. 779–790.

[6] Wang, Z., Wang, H., Mitra, A., Huang, L., and Yan, Y., 2001. "Pure-silica zeolite low-k dielectric thin films". *Advanced Materials,* ***13***(10), pp. 746 – 749.

[7] Davis, M., 2002. "Ordered porous materials for emerging applications". *Nature,* ***417***, pp. 813 – 821.

[8] Coronas, J., and Santamaria, J., 2004. "The use of zeolite films in small-scale and micro-scale applications". *Chemical Engineering Science,* ***59***(22-23), pp. 4879–4885.

[9] Dong, J., Zou, J., and Long, Y., 2003. "Synthesis and characterization of colloidal TBA-silicalite-2". *Microporous and Mesoporous Materials,* ***57***(1), pp. 9 – 19.

[10] Lai, Z., Bonilla, G., Diaz, I., Nery, J., Sujaoti, K., Amat, M., Kokkoli, E., Terasaki, O., Thompson, R., Tsapatsis, M., and Vlachos, D., 2003. "Microstructural optimization of a zeolite membrane for organic vapor separation". *Science,* ***300***(5618), pp. 456 – 460.

[11] Lew, C. M., Cai, R., and Yan, Y., 2009. "Zeolite thin films: From computer chips to space stations". *Accounts of Chemical Research,* ***43***(2), pp. 210–219.

[12] Liu, Z., Cacciola, G., Restuccia, G., and Giordano, N., 1990. "Fast simple and accurate measurement of zeolite thermal conductivity". *Zeolites,* ***10***(6), pp. 565–570.

[13] Griesinger, A., Spindler, K., and Hahne, E., 1999. "Measurements and theoretical modeling of the effective thermal conductivity of zeolites". *International Journal of Heat and Mass Transfer,* ***42***(23), pp. 4363–4374.

[14] Murashov, V. V., and White, M. A., 2002. "Thermal properties of zeolites: Effective thermal conductivity of dehydrated powdered zeolite 4A". *Materials Chemistry and Physics,* ***75***(1-3), pp. 178–180.

[15] Jakubinek, M. B., Zhan, B.-Z., and White, M. A., 2007. "Temperature-dependent thermal conductivity of powdered zeolite NaX". *Microporous and Mesoporous Materials,* ***103***(1-3), pp. 108–112.

[16] Greenstein, A., Graham, S., Hudiono, Y., and Nair, S., 2006. "Thermal properties and lattice dynamics of polycrystalline MFI zeolite films". *Nanoscale and Microscale Thermophysical Engineering,* ***10***(4), pp. 321–336.

[17] Hudiono, Y., Greenstein, A., Saha-Kuete, C., Olson, B., Graham, S., and Nair, S., 2007. "Effects of composition and phonon scattering mechanisms on thermal transport in MFI zeolite films". *Journal of Applied Physics,* ***102***(5), p. 053523.

[18] Coquil, T., Lew, C. M., Yan, Y., and Pilon, L., 2010. "Thermal conductivity of pure silica MEL and MFI zeolite thin films". *Journal of Applied Physics,* ***108***(4), p. 044902.

[19] Flanigen, E., Bennett, J., Grose, R., Cohen, J., Patton, R., and Kirchner, R., 1978. "Silicalite, a new hydrophobic crystalline silica molecular sieve". *Nature,* ***271***(5645), pp. 512–516.

[20] Tang, Z., Dong, J., and Nenoff, T., 2009. "Internal surface modification of MFI-type zeolite membranes for high selectivity and high flux for hydrogen". *Langmuir,* ***25***(9), 04, pp. 4848–4852.

[21] Li, S., Sun, J., Li, Z., Peng, H., Gidley, D., Ryan, E. T., and Yan, Y., 2004. "Evaluation of pore structure in pure silica zeolite MFI low-k thin films using positronium annihilation lifetime spectroscopy". *Journal of Physical Chemistry B,* ***108***(31), pp. 11689–11692.

[22] Lew, C. M., Liu, Y., Kisailus, D., Kloster, G. M., Chow, G., Boyanov, B., Sun, M., Wang, J., and Yan, Y., 2011. "Insight into on-wafer crystallization of Pure-Silica-Zeolite films through nutrient replenishment". *Langmuir,* ***27***(7), pp. 3283–3285.

[23] Cahill, D., 1990. "Thermal conductivity measurement from 30 to 750K: the 3ω method". *Review of Scientific Instru-*

ments, ***61***, pp. 802–808.

[24] Kimling, J., Martens, S., and Nielsch, K., 2011. "Thermal conductivity measurements using 1ω and 3ω methods revisited for voltage-driven setups". *Review of Scientific Instruments,* ***82***(7), p. 074903.

[25] Fang, J., Reitz, C., Brezesinski, T., Nemanick, E. J., Tolbert, S. H., and Pilon, L., 2011. "Thermal conductivity of highly-ordered mesoporous titania thin films from 30 to 320 K". *Journal of Physical Chemistry C,* ***115***(30), pp. 14606–14614.

[26] Callaway, J., 1961. "Low-temperature lattice thermal conductivity". *Physical Review,* ***122***(3), pp. 787–790.

[27] Boerio-Goates, J., Stevens, R., Hom, B. K., Woodfield, B. F., Piccione, P. M., Davis, M. E., and Navrotsky, A., 2002. "Heat capacities, third-law entropies and thermodynamic functions of SiO_2 molecular sieves from T = 0 K to 400 K". *Journal of Chemical Thermodynamics,* ***34***(2), pp. 205–227.

[28] Mukhopadhyay, A. B., Oligschleger, C., and Dolg, M., 2003. "Molecular dynamics investigation of vibrational properties of zeolite ZSM-5-based amorphous material". *Physical Review B,* ***68***(2), p. 024205.

[29] Katika, K. M., and Pilon, L., 2008. "The effect of nanoparticles on the thermal conductivity of crystalline thin films at low temperatures". *Journal of Applied Physics,* ***103***(11), p. 114308.

[30] Tien, C. L., Majumdar, A., and Gerner, F. M., 1998. *Microscale Energy Transport*. Taylor and Francis, Washington, DC.

[31] Lee, S., and Cahill, D., 1997. "Heat transport in thin dielectric films". *Journal of Applied Physics,* ***81***(6), pp. 2590 – 2595.

[32] Greenstein, A., Hudiono, Y., Graham, S., and Nair, S., 2010. "Effects of nonframework metal cations and phonon scattering mechanisms on the thermal transport properties of polycrystalline zeolite LTA films". *Journal of Applied Physics,* ***107***(6), p. 063518.

[33] Dong, J., Lin, Y. S., Hu, M. Z.-C., Peascoe, R. A., and Payzant, E. A., 2000. "Template-removal-associated microstructural development of porous-ceramic-supported MFI zeolite membranes". *Microporous and Mesoporous Materials,* ***34***(3), pp. 241–253.